ORIGINAL PAPER

Photosynthetic characteristics of marine aerobic anoxygenic phototrophic bacteria *Roseobacter* and *Erythrobacter* strains

Yuki Sato-Takabe · Koji Hamasaki · Koji Suzuki

Abstract A coastal *Roseobacter* strain of marine aerobic anoxygenic phototrophic bacteria (AAnPB) was isolated and phylogenetically determined. The strain OBYS 0001 was characterized by its physiological and biochemical properties with reference to the *Erythrobacter longus* type strain NBRC 14126. When grown in batch cultures, the growth curves of the both strains were similar. Cellular bacteriochlorophyll *a* concentrations of the strains reached the maxima in the stationary growth conditions. In vivo fluorescence excitation/optical density spectra between 470 and 600 nm for OBYS 0001 represented higher values than NBRC 14126. Variable fluorescence measurements revealed that the functional absorption cross section (σ) of the bacterial photosynthetic complexes for OBYS 0001 was significantly higher than that for NBRC 14126 under green excitation. These results suggest that *Roseobacter* can capture green light more efficiently than *Erythrobacter* for photosynthesis. The photochemical quantum efficiencies (F_v/F_m) of the bacterial photosynthetic complexes for OBYS 0001 were consistently lower than those for NBRC 14126. A relationship between the growth rate and F_v/F_m was significant for OBYS 0001, but that was not found for NBRC 14126. These results suggested that F_v/F_m for AAnPB could not be used as a proxy of the growth rate which is consistent with their mostly heterotrophic characters.

Keywords Aerobic anoxygenic phototrophic bacteria · *Roseobacter* · *Erythrobacter* · Variable fluorescence · Absorption · Excitation spectrum

Communicated by Joerg Overmann.

Y. Sato-Takabe (✉) · K. Suzuki
Graduate School of Environmental Science, Hokkaido University, North 10 West 5, Kita-ku, Sapporo 060-0810, Japan
e-mail: satoyuki@ees.hokudai.ac.jp

Y. Sato-Takabe · K. Hamasaki
Ocean Research Institute, The University of Tokyo, Tokyo, Japan

K. Suzuki
Faculty of Environmental Earth Science, Hokkaido University, Sapporo, Japan

Introduction

Aerobic anoxygenic phototrophic bacteria (AAnPB) are primarily heterotrophic organisms capable of harvesting light energy using photosynthetic reaction centers composed of bacteriochlorophyll *a* (BChl *a*; Yurkov and Csotonyi 2009). Therefore, their metabolic performance is called 'photoheterotrophy'. Recently, AAnPB and other photoheterotrophs including proteorhodopsin-containing bacteria and cyanobacterium *Prochlorococcus* have been classified into a new functional group in terms of energy acquisition (Béjà and Suzuki 2008). However, unlike cyanobacteria and eukaryotic phytoplankton, photoautotrophic CO_2 fixation is absent in all physiologically tested AAnPB, with both enzymological and full-genome sequence studies, confirming the lack of the key Calvin cycle enzyme ribulose-1,5-bisphosphate carboxylase/oxygenase (RubisCO) (Yurkov and Beatty 1998). On the other hand, Kolber et al. (2001) and Rathgeber et al. (2004) reported the low levels of AAnPB CO_2 fixation are thought to be a function of phosphoenolpyruvate (PEP) carboxylase, a key respiratory enzyme that replaces the organic acids sequestered from the citric acid cycle by other biochemical pathways (Yurkov and Csotonyi 2009).

From an ecological standpoint, AAnPB were first isolated from a variety of marine environments (i.e.,

seaweeds, beach sand, and seawater) using direct cultivation methods by Shiba et al. (1979). The contribution of AAnPB to bacterial populations ranged from 0.9 to 1.1% in seaweed, from 1.2 to 6.3% in sand, and 0.9% in seawater (Shiba et al. 1979), indicating that they possibly prefer organic matter-rich environments. Recently, Kolber et al. (2001) reported AAnPB comprised at least 11% of total bacterial abundance in the upper open ocean. Thereafter, it has become clear that AAnPB are widely distributed and their spatiotemporal changes are large in the upper oceans (Schwalbach and Furhman 2005; Jiao et al. 2007; Lami et al. 2007). However, what controls their population dynamics is an open question. Although the photosynthetic machinery of AAnPB has been gradually elucidated (Yurkov and Csotonyi 2009), less is still known about the physiological characteristics of AAnPB. For example, the contribution of photosynthesis to their growth has seldom been quantified. Koblížek et al. (2003) determined the biochemical and physiological characteristics of several *Erythrobacter* strains in terms of 16S rRNA and *pufM* gene sequences, growth rates, in vivo absorption and fluorescence excitation spectra, and pigment composition. More recently, Koblížek et al. (2010) revealed the photosynthetic properties of AAnPB belonging to *Roseobacter* clade (strain COL2P). However, those parameters for the other AAnPB have not yet been reported. Moreover, the differences in photosynthetic characteristics between *Roseobacter* and *Erythrobacter* remain unclear.

Here, we isolated coastal marine AAnPB bacteria belonging to the genus *Roseobacter* (strain OBYS 0001) and characterized physiological and biochemical properties, especially in photosynthesis, comparing them with those of the *Erythrobacter longus* type strain (NBRC 14126). The purpose of this study is to clarify similarity and dissimilarity in photosynthetic characteristics of two AAnPB genera, *Roseobacter* and *Erythrobacter*.

Materials and methods

Strain isolation

Approximately 200 μl of the seawater collected from the surface layer (1 and 5 m) of the Otsuchi Bay, NW Pacific (39°N, 141°E), was streaked onto 1/25 ZoBell 2216E agar plates, which was prepared with filtered seawater supplemented with 0.2 g peptone and 0.04 g yeast extract per liter. Plates were stored for 14 days at 20°C and thereafter for 14 days at room temperature, resulting in the production of small, pigmented colonies. The type strains, *Erythrobacter longus* strain NBRC 14126, *Roseobacter denitrificans* strain NBRC 15277, and *R. litoralis* strain NBRC 15278 also formed colonies under these conditions.

Some pigmented colonies were picked up, streaked onto new agar plates, and incubated for 7 days for isolation.

Phylogenetic analysis

Bacterial DNA was extracted from the colonies of *Roseobacter* sp. strain OBYS 0001 using a PrepMan sample preparation reagent (Perkin-Elmer–Applied Biosystems) and used for PCR amplification of the 16S rRNA gene (Herbst et al. 2001).

Methods for DNA purification, PCR amplification, and species identification have been described in Parvin and Nishino (2009). Amplification of the 16S rRNA gene was accomplished using a forward primer 27f (5′-AGAGT TTGATCCTGGCTCAG-3′) and a reverse primer 1492r (5′-GGCTACCTTGTTACGACTT-3′). Purified PCR products were sequenced using the Big Dye Terminator v3.1 Cycle Sequencing Kit (Applied Biosystems) in combination with the ABI PRISM 310A (Applied Biosystems) automated sequencing system. A Basic Local Alignment Search Tool (BLAST) program was used to determine closest relatives of the 16S rRNA gene sequence.

Incubation and cell counting

The *Roseobacter* sp. strain OBYS 0001 and *Erythrobacter longus* strain NBRC 14126 were grown in 2.8-L polycarbonate Erlenmeyer flasks in ZoBell 2216E medium (salinity = 33.0). Cells were grown at 20°C under light and dark cycles (12 h/12 h). Light from a fluorescent lamp was subdued to ca. 8 μmol photons m^{-2} s^{-1}, because our strain was obtained from turbid waters at 1 m. The time-course samples, which were collected daily at the end of the dark period, were filtered onto Nuclepore black polycarbonate membrane filters (0.2 μm in pore size) under gentle vacuum (≤0.025 MPa). Cells were counted using epifluorescence microscopy (Olympus CKX-41N-FI) with the SYBR Gold staining method (Shibata et al. 2006). A minimum of 10 randomly selected fields were examined, producing at least 300 bacterial cells.

Pigment analysis

Concentration of BChl *a* (Frontier Scientific) in methanol was determined spectroscopically with a Shimadzu MPS-2450 spectrophotometer using the absorption coefficient of $\varepsilon_{771} = 54.8$ mM^{-1} cm^{-1} (Permentier et al. 2000).

For examining the BChl *a* concentrations of the AAnPB strains by HPLC, all samples (1 ml each) were filtered onto GF/F filters (Whatman) under gentle vacuum (≤0.025 MPa) and sonicated with a Branson Sonifier Model 250 at 10 W for 50 s on ice. The pigment extracts were filtered through 0.45-μm PTFE filters. Samples

(250 μl) of a mixture of 250 μl 28 mM tetrabutylammonium acetate solution (pH 6.5) plus 250 μl pigment extract were injected into a CLASS-VP HPLC system with a Zorbax Eclips XD8-C8 column (4.6 × 150 mm). A binary solvent system was employed for the HPLC pigment analysis following Van Heukelem and Thomas (2001): solvent A (methanol: 28 mM tetrabutylammonium acetate solution at pH 6.5, 70:30, v:v) and solvent B (methanol). The flow rate was held constant at 1.2 ml min^{-1}. Pigment separation was made by the linear gradient of 5–95% B in 22 min followed by an isocratic hold at 95% B for 8 min. Column temperature was kept at 60°C. The peak of BChl a was identified by a Shimadzu photodiode array detector and by comparison of the retention times with the authentic standard of BChl a (Frontier Scientific).

For estimating the pigment compositions of the AAnPB strains by HPLC, the cell pellets collected by centrifugation were placed in 3 ml methanol and sonicated with a Branson Sonifier Model 250 at 10 W for 50 s on ice. The pigment extracts were filtered through 0.45-μm PTFE filters and analyzed by HPLC with the same procedure described above. Standards were obtained from commercial products for BChl a (Frontier Scientific) and zeaxanthin (Extrasynthese). For spheroidenone, erythroxanthin sulfate, and bacteriorubixanthinal, standards were obtained from the extracts of the AAnPB strains purified by a Shimadzu semi-preparative HPLC system. The carotenoids collected were transferred into 100% methanol, and the absorption spectra were compared to those published previously (Koblížek et al. 2003, 2010).

FIRe fluorometry

The photosynthetic ability of the bacterial isolates was assessed using the FIRe (Fluorescence Induction and Relaxation) fluorometer (Satlantic Inc., Canada), in which blue (455 nm with 60 nm bandwidth) and green (540 nm with 60 nm bandwidth) light-emitted diodes (LEDs) were incorporated. The FIRe protocol involved a strong flash of saturating blue and green, initiating a rise in fluorescence in vivo from an initial value (F_0) to the maximum value (F_m) in a single-turnover flash. A strong short pulse of 80-μs duration (i.e., single-turnover flash) induced transient changes in the BChl a fluorescence emission at 880 nm. Before measurements, samples were dark-adapted for 30 min to open the reaction centers. Triplicate samples were measured with 10 iterations per sample. Then, ZoBell 2216E medium was used as a blank for the sample signals. Raw data were collected following the manufacturer protocol and processes with the MATLAB-based program fireworx developed by Dr. Audrey B. Barnett (Dalhousie Univ.) for obtaining F_v/F_m and σ (the maximum photochemical quantum efficiency and functional absorption

cross section of the bacterial photosynthetic complexes, respectively) and τ (time constant for Q_a reoxidation). τ was estimated from the first component (τ_1) of the three exponential decay models of Kolber et al. (1988).

Absorption and fluorescence excitation properties

Because of the low absorbance of AAnPB in the medium, the absorption properties were assessed by the quantitative filter technique of Kishino et al. (1985). In brief, water samples (1 ml) were filtered onto 25-mm Whatman GF/F glass-fiber filters under low vacuum pressure (≤0.025 MPa). Optical densities of AAnPB on the filter, $OD_f(\lambda)$, were measured using a spectrophotometer (Shimadzu MPS-2450) equipped with an end-on type photomultiplier tube. A blank filter, wetted with ZoBell 2216E medium solution onto 25-mm Whatman GF/F glass-fiber filters, was used as a reference. Spectral value of the absorption coefficient was recorded every 1 nm from 400 to 900 nm. All spectra were set to zero at 900 nm to minimize differences between sample and reference filters, assuming the lack of absorption at 900 nm. Measured $OD_f(\lambda)$ values were converted to the optical density in suspension (OD_s) using the following equations (cf. Cleveland and Weidemann 1993) which corrected increases in pathlength caused by multiple scattering in the glass-fiber filter and unknown factors:

$$OD_s = 1.30\, OD_f - 1.18\, OD_f^2 \qquad (1)$$
$$(r = 0.84) \text{ for OBYS } 0001$$

$$OD_s = 0.0436\, OD_f + 1.78\, OD_f^2 \qquad (2)$$
$$(r = 0.96) \text{ for NBRC } 14126$$

Another aliquot of the water samples was also used for measurement of BChl a fluorescence excitation spectra by a spectrofluorometer (Shimadzu RF-5300PC) equipped with a red-sensitive photomultiplier tube (Hamamatsu R928). The setting was made at an emission wavelength of 875 nm, with a resolution of 1 nm, using 5-nm excitation and 20-nm emission slit-widths. For the fluorescence excitation spectra, the cells were resuspended in 50% glycerol in ZoBell 2216E medium in order to intensify BChl a fluorescence (cf. Wyman 1992). The emission monochromator was protected against stray light by a Hoya IR83 glass filter. The excitation spectra obtained were corrected by quantum counter Basic Blue 3 (Kopf and Heinze 1984). Fluorescence/optical density ratios were calculated using the normalized excitation spectra by coinciding with their maxima between 400 and 650 nm. In vivo fluorescence emission spectra (350–700 nm) were also measured by the Shimadzu RF-5300PC spectrofluorometer. The setting was made at a fluorescence wavelength excited at 375 nm, with a resolution of 1 nm, using 5-nm excitation and 20-nm emission slit-widths.

Results

Isolation and phylogenetic analysis

A strain (OBYS 0001) containing BChl *a* was successfully isolated from seawater of the Otsuchi Bay. The in situ seawater temperature and salinity ranged from 9.5 to 11.8°C and from 32.8 to 33.2, respectively.

Phylogenetic analysis using 16S rRNA gene sequences revealed a close genetic relationship between the OBYS 0001 strain (GenBank Accession No. AB586070) and all species previously described as members of the genus *Roseobacter* in the α-3 subclass of *Proteobacteria* (Yurkov and Csotonyi 2009). The OBYS 0001 showed 99% similarity to *Roseobacter litoralis*. There was a distinct difference between the strain COL2P described by Koblížek et al. (2010) and our strain OBYS 0001. Although both strains belong to the *Roseobacter* clade (*Rhodobacterales* in *Alphaproteobacteria*), COL2P was phylogenetically closer to *Maritimibacter alkaliphilus* strain HTCC2654 (95%) than to *Roseobacter litoralis* and *R. denitrificance* (92%) (Fig. 1). It should be noted that the phylogenetic tree was constructed with a certain region of 16S rRNA gene (1,185 bp) because the full-length sequences of the gene were not available from some strains. The nucleotide sequences were aligned using the program Clustal W (Larkin et al. 2007) and edited manually. The phylogenetic trees were constructed with the neighbor-joining method of MEGA 4 (Tamura et al. 2007).
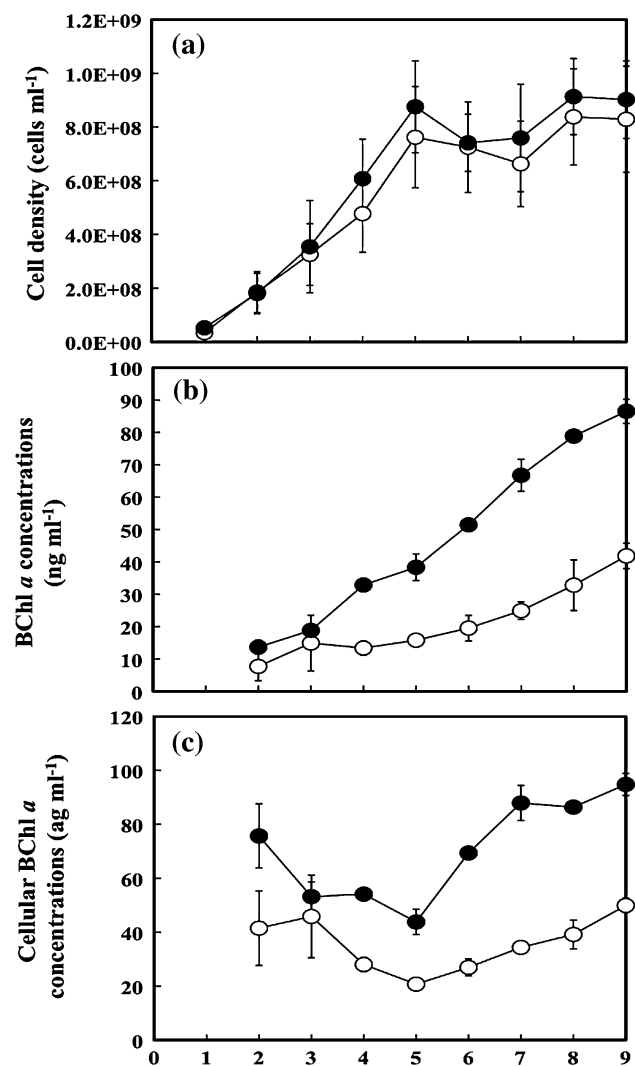

Fig. 1 A phylogenetic tree of 16S rRNA gene sequences among AAnPB. *Scale bar* 0.02–bp substitution per nucleotide position. Note that the phylogenetic tree was constructed with a certain region of 16S rRNA gene because the full-length sequence of the gene was not available from some strains
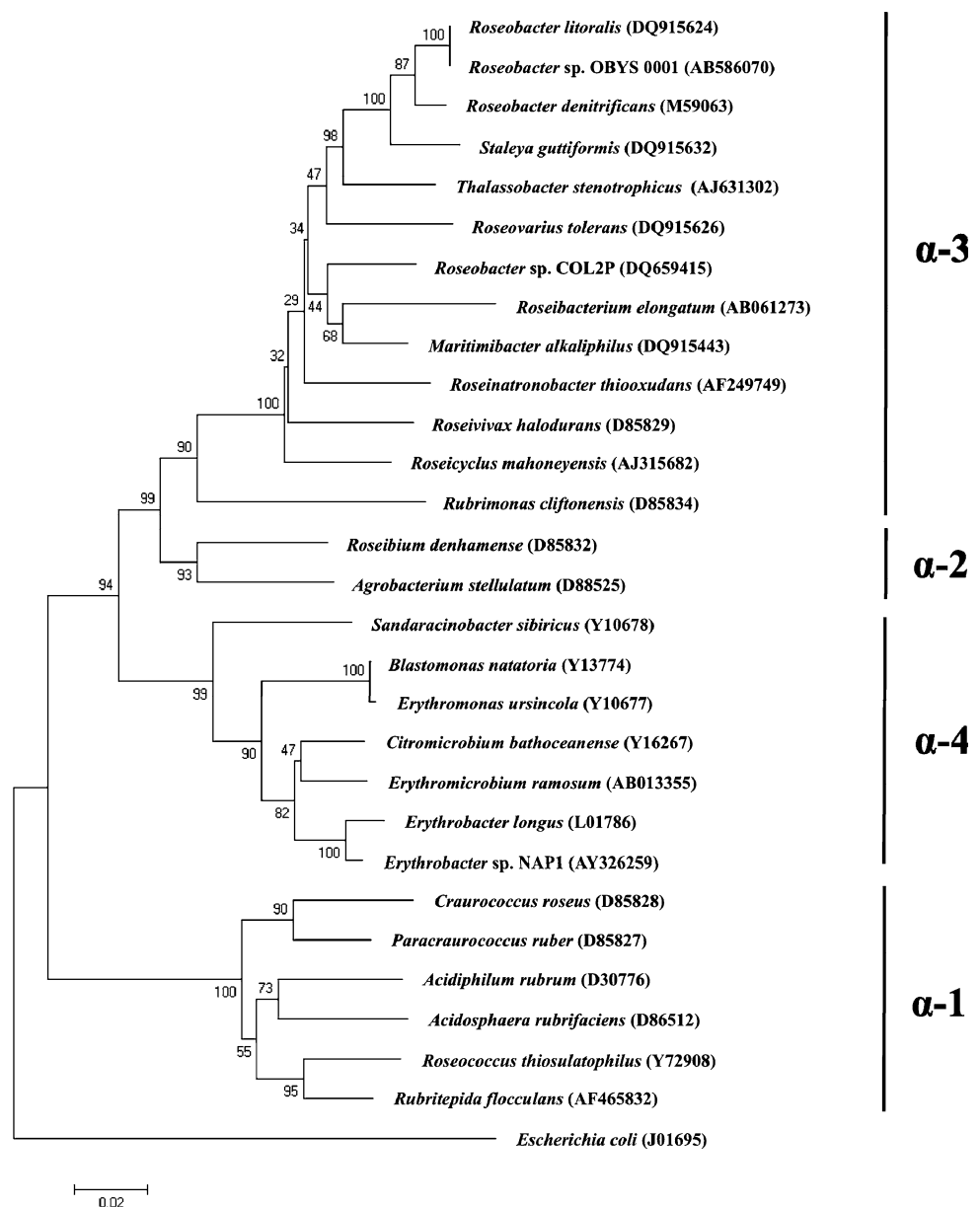
Cell growth and pigmentation

Cell densities increased from 3×10^7 to 8×10^8 cells ml^{-1} for NBRC 14126 and from 5×10^7 to 9×10^8 cells ml^{-1} for OBYS 0001 (Fig. 2a). Specific maximum growth rates (μ_{max}) of the two strains ranged from 1.4 to 1.9 day^{-1} (Table 1). BChl a concentrations of both strains gradually increased during experiments (Fig. 2b). The maxima of the cellular BChl a contents of the two strains were found in the stationary growth phases (Fig. 2c). The BChl a contents ranged from 21 to 50 ag per cell for NBRC 14126 and from 44 to 95 ag per cell for OBYS 0001 (Table 1). The cellular BChl a concentration of OBYS 0001 was generally higher than that of NBRC 14126 (Fig. 2c).

The maximum absorption wavelengths of each pigment in the two strains are summarized in Table 2. The OBYS 0001 possessed spheroidenone as a major carotenoid, while the NBRC 14126 had erythroxanthin sulfate, bacterioru-bixanthinal, and zeaxanthin. The maximum absorption wavelengths observed in this study slightly differed from the data of Koblížek et al. (2003, 2010), and those were probably caused by the differences between organic solvents, in which each pigment was dissolved.

Characteristics of variable fluorescence

Single-turnover flash saturation profiles of variable fluorescence using the blue and green excitations revealed that the functional absorption cross section (σ) of the bacterial photosynthetic complexes for OBYS 0001 was clearly higher than those of NBRC 14126 as measured by the green excitation (Fig. 3b), although in case of the blue excitation this pattern was ambiguous (Fig. 3a). The photochemical quantum efficiencies (F_v/F_m) of the photosystem for NBRC 14126 were consistently higher than those of OBYS 0001 throughout the experiment. The maxima of F_v/F_m for the two strains were found in their exponential growth phases (Fig. 3c, d). For OBYS 0001, higher σ values were observed in the exponential growth phase. For the reoxidation constant (τ) of Q_a^- (Fig. 3e, f), relatively high values were observed on days 3 and 9 for OBYS 0001 and between days 7–9 for NBRC 14126.

Optical density and fluorescence excitation properties

The in vivo optical density spectrum of OBYS 0001 exhibited two infrared Q_Y bands of BChl a, the large band between 801 and 813 nm and the smaller band at 856–872 nm in the near-infrared region (Fig. 4a). The large band between 801 and 813 nm (B806) indicated the presence of the light-harvesting complex 2 (LH2) and the smaller one between 856 and 872 nm in the presence of light-harvesting complex 1 (LH1) (Koblížek et al. 2003). On the other hand, NBRC 14126 possessed a single Q_Y band (864–875 nm; Fig. 4b) derived from RC-B865 complex of LH1 (Shimada et al. 1985). In the blue region, OBYS 0001 showed two distinct peaks, mainly derived from cytochromes, between 411 and 416 nm, but these bands were rather indistinct in NBRC 14126. A relatively high optical density between 450 and 550 nm, principally owing to carotenoids, was observed for NBRC 14126. Fluorescence excitation spectra of OBYS 0001 and NBRC 14126 were similar to each other (Fig. 4c, d), but several peaks were found between 450 and 600 nm for NBRC 14126. In vivo fluorescence excitation/optical density spectra (Fig. 4e, f) revealed that higher values were observed between 470 and 600 nm for OBYS 0001 and between 570 and 620 nm for NBRC 14126.

Fig. 2 Changes over time in the **a** cell densities, **b** BChl a concentration, and **c** cellular BChl a levels of OBYS 0001 (*filled circle*) and NBRC 14126 (*open circle*)

Table 1 Comparisons among the physiological characteristics of AAnPB strains

Organism	Bchl a (ag cell^{-1})	μ_{max}	F_v/F_m	σ_{blue}	σ_{green}	σ_{795}	LH1	LH2	References
Erythrobacter sp. strain NAP1	30–70	2.3 (20°C)	0.80–0.85	40–45 (470 nm)	n.d.	n.d.	+	–	Koblížek et al. (2003)
Roseobacter sp. strain COL2P	39–248	n.d.	~0.7	n.d.	n.d.	n.d.	+	–	Koblížek et al. (2010)
Roseobacter denitrificans strain DSM 7001	n.d.	n.d.	0.75 ± 0.01	n.d.	95 ± 5 (530 nm)	n.d.	+	+	Tang et al. (2010)
Rhodobacter sphaeroides strain 8253	n.d.	n.d.	0.82 ± 0.01	69 ± 2 (470 nm)	n.d.	82 ± 2 (795 nm)	+	+	Koblížek et al. (2005)
Rhodobacter sphaeroides strain M21	n.d.	n.d.	0.77 ± 0.01	28 ± 1 (470 nm)	n.d.	~0	+	–	Koblížek et al. (2005)
Rhodobacter capsulatus strain pTB9991	n.d.	n.d.	0.81 ± 0.01	106 ± 3 (470 nm)	n.d.	100 ± 2 (795 nm)	+	+	Koblížek et al. (2005)
Rhodospirillum rubrum strain S1	n.d.	n.d.	0.74 ± 0.01	16 ± 1 (470 nm)	n.d.	~0	+	–	Koblížek et al. (2005)
Roseobacter sp. strain OBYS 0001	44–95	1.4 (20°C)	0.50–0.58	49–67 (455 nm)	74–104 (540 nm)	n.d.	+	+	This study
Erythrobacter longus strain NBRC 14126	21–50	1.9 (20°C)	0.60–0.68	53–61 (455 nm)	58–67 (540 nm)	n.d.	+	–	This study

σ_{blue}, σ_{green}, and σ_{795} represent σ values obtained by the blue, green, and red excitations, respectively

n.d. no data

Discussion

Phylogenetic analysis

We successfully isolated an AAnPB strain showing 99% similarity to *Roseobacter litoralis* NBRC 15278 from Otsuchi Bay, Japan, and demonstrated its photosynthetic characteristics in comparison with *Erythrobacter* sp. In rDNA clone libraries, *Erythrobacter* clade has rarely been reported in marine environments (Béjà and Suzuki 2008), while *Roseobacter* clade has often been documented (e.g., Buchan et al. 2005). Cottrell et al. (2006) also found that the bulk of the AAnPB detected above 200 m of the Mid-Atlantic Bright and the central North Pacific Gyre were not members of *Erythrobacter* as estimated by fluorescence in situ hybridization (FISH) and infrared fluorescence microscopy. These studies indicated that *Erythrobacter* species might not represent the predominant AAnPB in the upper oceans and that more detailed study of the ecologically important *Roseobacter* species in AAnPB is essential for better understanding of the ecology and physiology of the organisms. Koblížek et al. (2003) reported, for the first time, photosynthetic characteristics of *Erythrobacter* sp. strains in marine AAnPB. Koblížek et al. (2010) also reported photosynthetic characteristics of another AAnPB isolate, the COL2P strain. Phylogenetic analysis of 16S rRNA gene sequences showed a distinct difference between our isolate OBYS 0001 strain and the COL2P strain (see Fig. 1). Although both strains belong to the *Roseobacter* clade (*Rhodobacterales* in *Alphaproteobacteria*) and possess a photosynthetic pigment BChl *a*, the COL2P strain showed the highest similarity to the bacterium *Maritimibacter alkaliphilus* strain HTCC2654.

Photosynthetic characteristics

BChl *a* concentrations (Fig. 2b) of OBYS 0001 and NBRC 14126 strains increased from the exponential to the stationary phases determined from their cell densities (Fig. 2a). Interestingly, cellular BChl *a* content in both strains showed minima on day 5 corresponding to the end of the exponential growth phase, and the highest cellular BChl *a* content was observed at the end of the experiment (i.e., day 9), representing the high production of BChl *a* at the stationary growth phase (Fig. 2c). The results are consistent with those of Shiba and Harashima (1986) who showed that AAnPB produced BChl *a* after the exponential growth stage. The cellular BChl *a* levels of OBYS 0001 and NBRC 14126 were 44–95 and 21–50 ag cell^{-1}, respectively. The lowest value (21 ag cell^{-1}) of NBRC 14126 was the minimum among the data published previously (see Table 1). Recently, Koblížek et al. (2010) reported that cellular BChl *a* content of strain COL2P

Table 2 Retention time and absorption properties of major pigments detected in OBYS 0001 and NBRC 14126 in HPLC eluent

R_t (min)	Pigment identification	Observed λ_{max} (nm)	Published λ_{max} (nm)
10.5	Erythroxanthin sulfate	472	469
17.1	Bacteriorubixanthinal	510	510
18.5	Zeaxanthin	450, 478	(482), 454, 481
20.0	Canthaxanthin	475–477	475
20.6	Canthaxanthin derivative	463–465	–
24.6	Spheroidenone	481	485
22.8	Bacteriochlorophyll *a*	372, 590, 770	358, 577, 773

Published data were cited Takaichi et al. (1991)

Fig. 3 For OBYS 0001 (*filled circle*) and NBRC 14126 (*open circle*), changes over time in the functional absorption cross section (σ) of the bacterial photosynthetic complexes estimated by the **a** blue or **b** green excitations of FIRe fluorometer, the photochemical quantum efficiency (F_v/F_m) of the bacterial photosynthetic complexes estimated by the **c** blue or **d** green excitations and the time constant (τ) for Q_a^- reoxidation estimated by the **e** blue or **f** green excitations
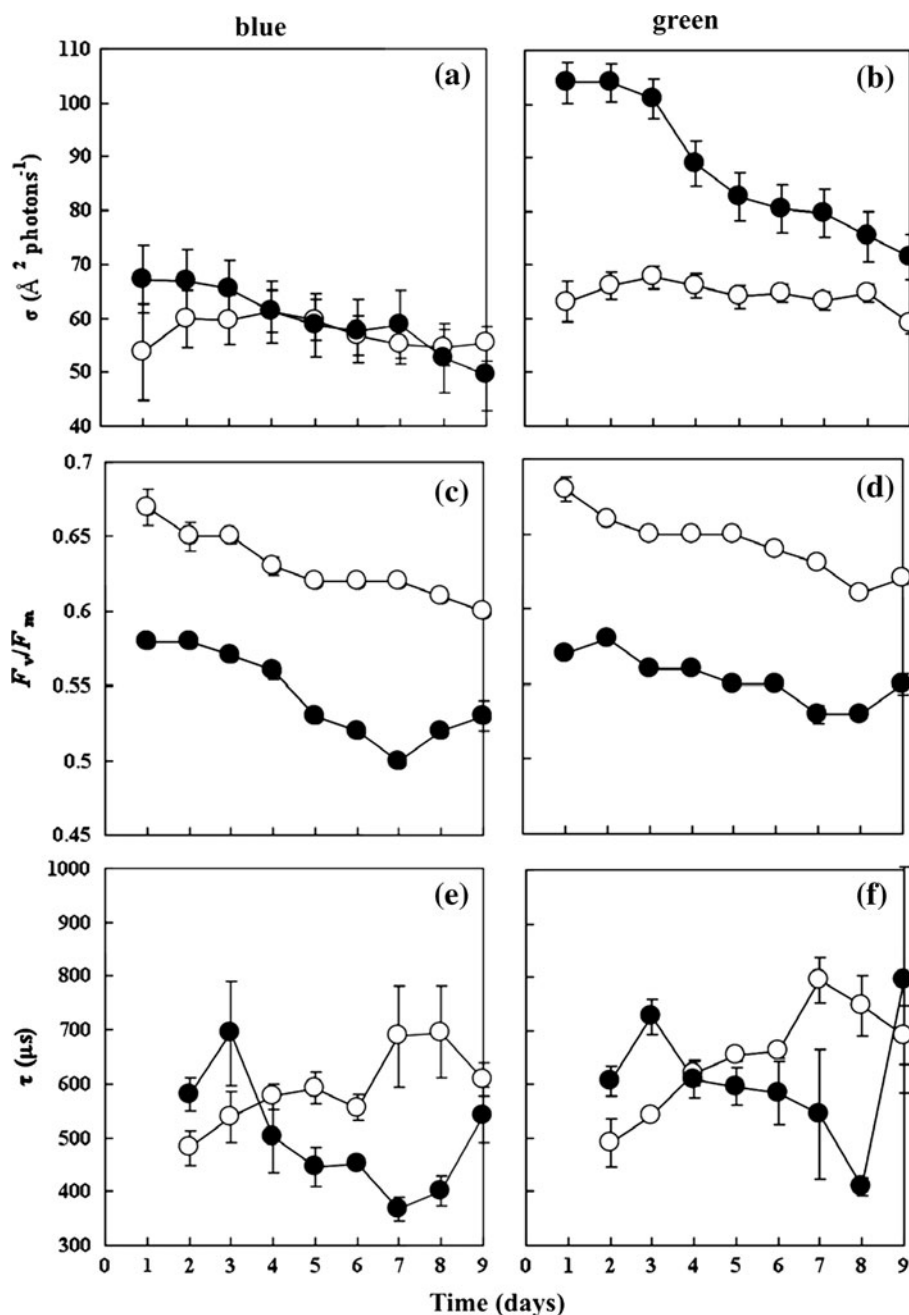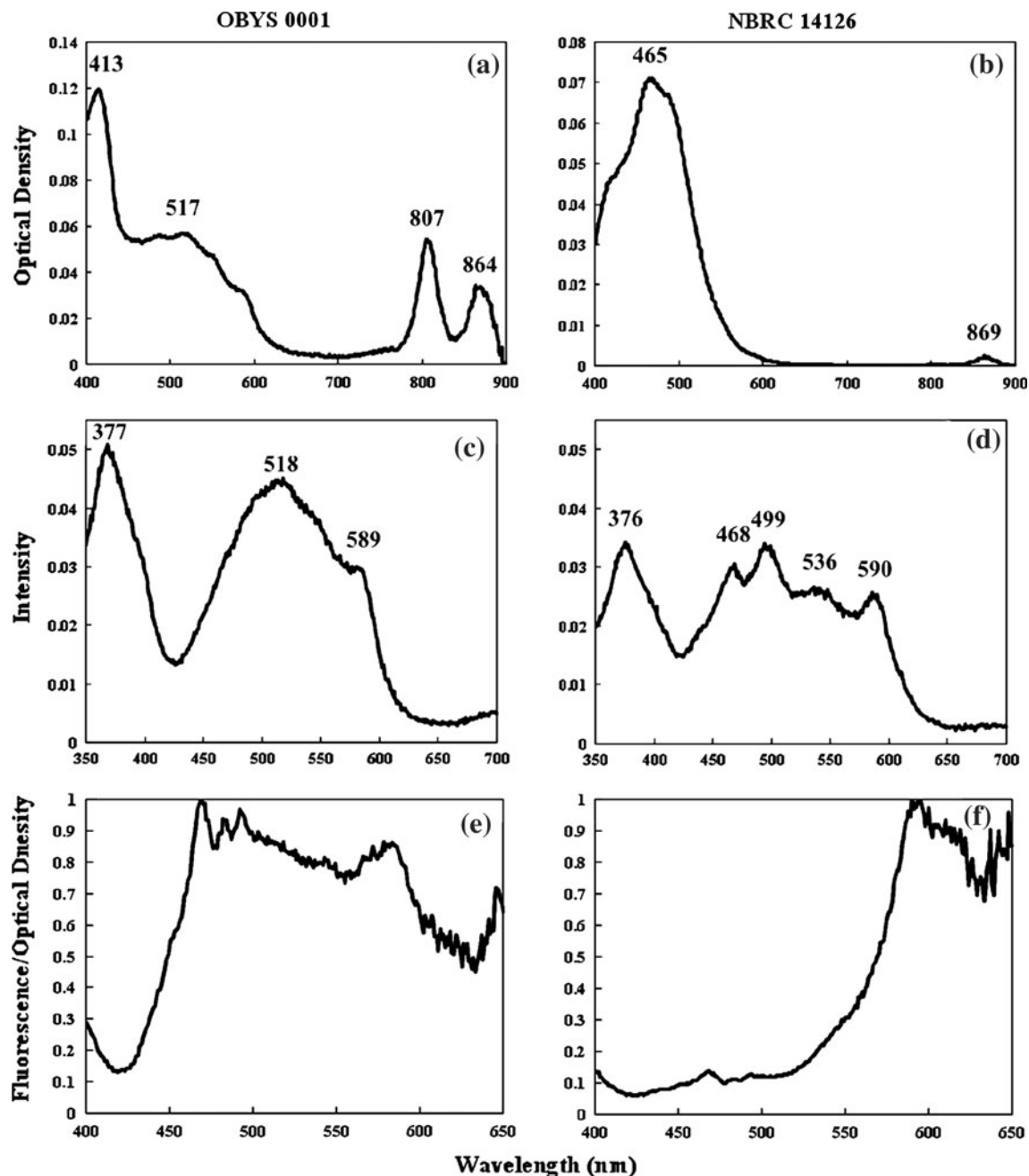
Fig. 4 Spectra of **a**, **b** in vivo optical density, **c**, **d** fluorescence excitation, and **e**, **f** fluorescence normalized to optical density between 350 nm and 700 nm of OBYS 0001 (*left panels*) and NBRC 14126 (*right panels*)

increased clearly under a P-limited condition. These results including our study indicate that the synthesis of BChl *a* in AAnPB is upregulated under nutrition-replete conditions.

Unlike *Erythrobacter* species reported by Koblížek et al. (2003) and this study, *Roseobacter* sp. OBYS 0001 possessed only one major carotenoid, spheroidenone. Similarly, the pigment was the sole carotenoid in strain COL2P (Koblížek et al. 2010). Spheroidenone was also found in *Roseobacter denitrificans* and *Roseobacter litoralis* as well as other AAnPB species belonging to *Roseobacter* clade

(Wagner-Dobler and Biebl 2006). These results suggest that spheroidenone can be useful as a possible indicator of AAnPB in *Roseobacter* clade, and the pigment can play a major role in light-harvesting antenna (Koblížek et al. 2010). The result is also consistent with that of the fluorescence/optical density spectra (Fig. 4e, f) showing the higher values of OBYS 0001 between 470 and 600 nm where the absorption bands of spheroidenone and BChl *a* are covered. On the other hand, NBRC 14126 possessed three major carotenoids, erythroxanthin sulfate,

bacteriorubixanthinal, and zeaxanthin. The pigment composition is consistent with the results of *Erythrobacter longus* ATCC 339341 (Takaichi et al. 1988, 1990, 1991). The highly polar carotenoid, erythroxanthin sulfate, is considered to be not associated with the RC-B865 BChl–protein complex (Shimada et al. 1985), demonstrating that the pigment is non-photosynthetic. Noguchi et al. (1992) reported that bacteriorubixanthinal and zeaxanthin were photosynthetic carotenoids and were conjugated to the RC-B865 complex with a high-energy transfer efficiency to BChl a ($88 \pm 5\%$). The results are consistent with the fluorescence excitation spectrum of NBRC 14126 (Fig. 4d) showing higher values between 470 and 600 nm. Koblížek et al. (2003) also showed similar results using *Erythrobacter* sp. NAP1. It is known that erythroxanthin sulfate is the most dominant carotenoid in the membrane of *E. longus* (>70%) (Noguchi et al. 1992). This could lead to the lower fluorescence excitation/optical density ratios between 470 and 600 nm for NBRC 14126, compared to OBYS 0001 (Fig. 4e, f).

Although AAnPB seem to increase BChl a cellular content under suboptimal growth conditions as mentioned above, F_v/F_m of OBYS 0001 and NBRC 14126 tended to decrease toward the end of the experiment (Fig. 3c, d), suggesting a decline of photosynthetic activity with a decrease in nutrition. F_v/F_m values for OBYS 0001 were consistently lower than those for NBRC 14126 under blue or green excitations, although their growth rates were not significantly different (Fig. 2a). For phytoplankton, F_v/F_m is often used for a diagnostic marker of nitrogen and/or iron deficiency and for a proxy of growth rate (e.g., Parkhill et al. 2001; Suzuki et al. 2002; Boyd et al. 2005). A decrease in F_v/F_m is observed once nutrient availability decreases relative to the cellular demand for photosynthesis, and the algal growth rate inevitably declines (see

Parkhill et al. 2001). A relationship between the growth rate and F_v/F_m under the blue and green excitations was significant for OBYS 0001 ($P < 0.05$, $n = 8$, Spearman two-tailed test), although that was not found for NBRC 14126 (Fig. 5). These results suggested that, unlike phytoplankton, F_v/F_m for AAnPB could not be simply used for a proxy of their growth rate, and the uncertainty was probably caused by their heterotrophy. Koblížek et al. (2003) pointed out that the growth of AAnPB relied exclusively on organic carbon substrates.

The σ values (74–104 Å^2 per quanta) of OBYS 0001 were clearly higher than those (58–67 Å^2 per quanta) of NBRC14126 as measured by the green excitation, representing that OBYS 0001 absorbed green light more efficiently than NBRC 14126 for photosynthesis. The results are consistent with the fluorescence excitation/optical density spectrum (Fig. 4e, f) showing the higher values of OBYS 0001 between 470 and 600 nm. Recently, Tang et al. (2010) also showed relatively high σ values (90–100 Å^2 per quanta) of *Roseobacter denitrificans* DSM 7001 strain using the green excitation of FIRe fluorometer. The higher σ in *Roseobacter* than *Erythrobacter* may be related to the presence of light-harvesting complex 2 (LH2) in *Roseobacter* and the absence of LH2 in *Erythrobacter* as described above. On the other hand, σ values of OBYS 0001 measured by the blue excitation were relatively low, and those were similar to the values obtained by blue excitations in the past studies (Table 1).

The F_v/F_m values were not significantly correlated with σ in both strains ($P > 0.05$, $n = 54$, $r = 0.52$ for *Roseobacter*, and $P < 0.05$, $n = 54$, $r = 0.42$ for *Erythrobacter*; Fig. 6), indicating that the activities of reaction centers and antenna systems were not closely coupled in AAnPB. In addition, any significant relationships between the cellular BChl a concentrations and variable

Fig. 5 Relationships between the growth rate (μ) and F_v/F_m for OBYS 0001 (*filled circle*) and NBRC 14126 (*open circle*). Estimated by the **a**, **c** blue or **b**, **d** green excitations of FIRe fluorometer
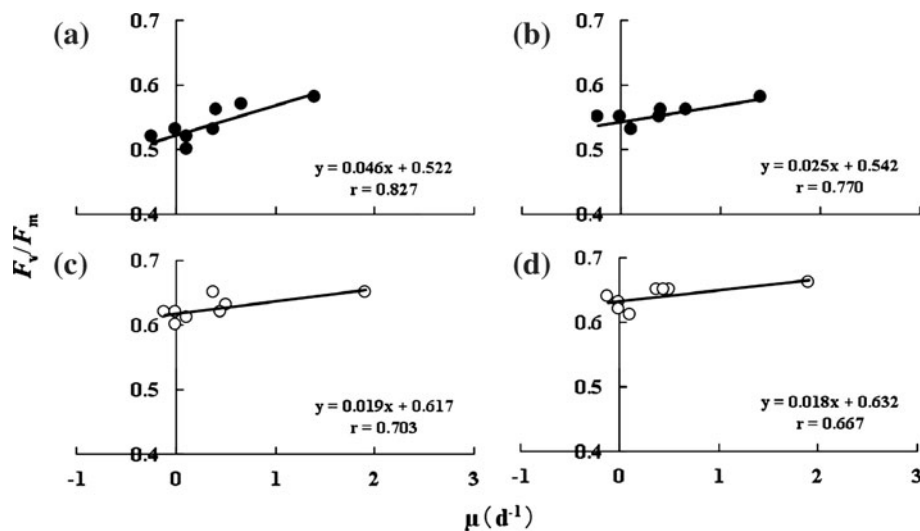
Fig. 6 Relationships between F_v/F_m and σ under blue and green excitations for **a** OBYS 0001 (*filled circle*) and **b** NBRC 14126 (*open circle*)
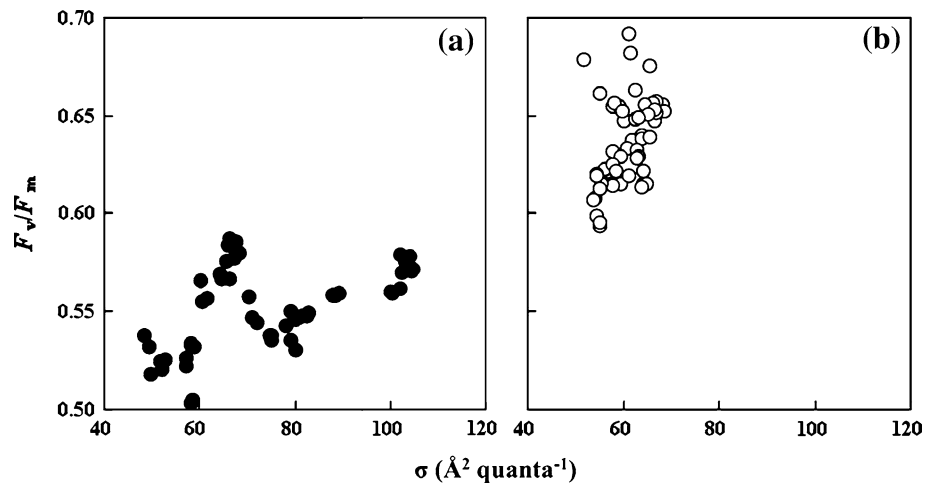
fluorescence parameters were not found (data not shown), suggesting that cellular BChl *a* content did not directly reflect the photosynthetic competence of AAnPB. However, Suyama et al. (2002) reported that BChl *a* synthesis and the expression of the *pufM* gene encoding the photosynthetic reaction center subunit M were stimulated under carbon-limited conditions. Additional studies are needed for clarifying the relationships between the variable fluorescence parameters, BChl *a*, and their controlling factors.

In this study, the similarities and dissimilarities of photosynthetic characteristics between the *Roseobacter* and *Erythrobacter* species have been clarified. AAnPB have an ability to supplement a significant fraction of their metabolic requirements with photosynthetically driven ATP production, as indicated by a strong suppression of respiration under irradiance (Koblížek et al. 2003). Further studies are also required to confirm whether or not the differences in photosynthetic characteristics between *Roseobacter* and *Erythrobacter* make for dissimilarities in their photoheterotrophic activities.

References

Béjà O, Suzuki MT (2008) Photoheterotrophic marine prokaryotes. In: Kirchman DL (ed) Microbial ecology of the ocean. Wiley, pp 131–158

Boyd PW, Strzepek R, Takeda S, Jackson G, Wong CS, McKay RM, Law C, Kiyosawa H, Saito H, Sherry N, Keith J, Gower J, Ramaiah N (2005) The evolution and termination of an iron-induced mesoscale bloom in the northeast subarctic Pacific. Limnol Oceanogr 50:1872–1886

Buchan A, Gonzalez JM, Moran MA (2005) Overview of the marine *Roseobacter* lineage. Appl Environ Microbiol 71:5665–5677

Cleveland JS, Weidemann AD (1993) Quantifying absorption by aquatic particles: a multiple scattering correction for glass-fiber filters. Limnol Oceanogr 38:1321–1327

Cottrell MT, Mannino A, Kirchman DL (2006) Aerobic anoxygenic phototrophic bacteria in the Mid-Atlantic Bright and the North Pacific Gyre. Appl Environ Microbiol 72:557–564

Herbst LH, Costa SF, Weiss LM, Johnson LK, Bartell J, Davis R, Walsh M, Levi M (2001) Granulomatous skin lesions in moray eels caused by a novel *Mycobacterium* species related to *Mycobacterium triplex*. Infect Immun 69:4639–4646

Jiao N, Zang Y, Zeng Y, Hong N, Liu R, Chen F, Wang P (2007) Distinct distribution pattern of abundance and diversity of aerobic anoxygenic phototrophic bacteria on the sea. Environ Microbiol 9:3091–3099

Kishino M, Takahashi M, Okami N, Ichimura S (1985) Estimation of the spectral absorption coefficients of phytoplankton in the sea. Bull Mar Sci 37:634–642

Koblížek M, Béjà O, Bidigare RR, Christensen S, Benetiz-Nelson B, Vetriani C, Kolber MK, Falkowski PG, Kolber ZS (2003) Isolation and characterization of *Erythrobacter* sp. strains from the upper ocean. Arch Microbiol 180:327–338

Koblížek M, Shih JD, Breirbart SI, Ratcliffe EC, Kolber ZS, Hunter CN, Niederman RA (2005) Sequential assembly of phototrophic units in *Rhodobacter sphaeroides* as revealed by fast repetition rate analysis of variable bacteriochlorophyll *a* fluorescence. Biochemi Biophys Acta 1706:220–231

Koblížek M, Mlčoušková J, Kolber Z, Kopecký J (2010) On the photosynthetic properties of marine bacterium COL2P belonging to *Roseobacter* clade. Arch Microbiol 192:41–49

Kolber Z, Zehr J, Falkowski P (1988) Effect of growth irradiance and nitrogen limitation on photosynthetic energy conversion in photosystem II. Plant Physiol 88:923–929

Kolber ZS, Plumley FG, Lang AS, Beatty JT, Blankenship RE, VanDover CL, Vetriani C, Koblížek M, Rathgeber C, Falkowski PG (2001) Contribution of aerobic photoheterotrophic bacteria to the carbon cycle in the ocean. Science 292:2492–2495

Kopf U, Heinze J (1984) 2,7-Bis (diethylamino) phenazoxonium chloride as a quantum counter for emission measurements between 240 and 700 nm. Anal Chem 56:1931–1935

Lami R, Cottrell MT, Ras J, Ulloa O, Obernosterer I, Claustre H, Kirchman DL, Lebaron P (2007) High abundances of aerobic anoxygenic photosynthetic bacteria in the South Pacific Ocean. Appl Environ Microbiol 73:4198–4205

Larkin MA, Blackshields G, Brown NP, Chenna R, McGettigan PA, McWilliam H, Valentin F, Wallace IM, Wilm A, Lopez R, Thompson JD, Gibson TJ, Higgins DG (2007) Clustal W and Clustal X version 2.0. Bioinformatics 15:87–88

Noguchi T, Hayashi H, Shimada K, Takaichi S, Tasumi M (1992) In vivo states and functions of carotenoids in an aerobic photosynthetic bacterium, *Erythrobacter longus*. Photosynth Res 31:21–30

Parkhill J-P, Maillet G, Cullen JJ (2001) Fluorescence-based maximal quantum yield for PSII as a diagnostic of nutrient stress. J Phycol 37:517–529

Parvin S, Nishino N (2009) Bacterial community associated with ensilage process of wilted guinea grass. J Appl Microbiol 107:2029–2036

Permentier HP, Schmidt KA, Kobayashi M, Akiyama M, Hager-Braun C, Neerken S, Miller M, Amesz J (2000) Composition and optical properties of reaction centre core complexes from green sulfur bacteria *Prosthecochloris aestuarii* and *Chlorobium tepidum*. Photosynth Res 64:27–39

Rathgeber C, Beatty JT, Yurkov V (2004) Aerobic phototrophic bacteria: a new evidence for the diversity, ecological importance and applied potential of this previously overlooked group. Photosynth Res 81:113–128

Schwalbach MS, Furhman JA (2005) Wide ranging abundances of aerobic anoxygenic phototrophic bacteria in the world ocean revealed by epifluorescence microscopy and quantitative PCR. Limnol Oceanogr 50:620–628

Shiba T, Harashima K (1986) Aerobic phototrophic bacteria. Molecul Microbiol 3:376–378

Shiba T, Shimidu U, Taga N (1979) Distribution of aerobic bacteria which contain bacteriochlorophyll a. Appl Environ Microbiol 38:43–45

Shibata A, Goto Y, Saito H, Kikuchi T, Toda T, Taguchi S (2006) Comparison of SYBR Green I and SYBR Gold stains for enumerating bacteria and viruses by epifluorescence microscopy. Aquat Microb Ecol 43:223–231

Shimada K, Hayashi H, Tasumi M (1985) Bacteriochlorophyll-protein complexes of aerobic bacteria, *Erythrobacter longus* and *Erythrobacter* species OCh 114. Arch Microbiol 143:244–247

Suyama T, Shigematsu T, Suzuki T, Tokiwa Y, Kanagawa T, Nagashima KVP, Hanada S (2002) Photosynthetic apparatus in *Roseateles depolymerans* 61A is transcriptionally induced by carbon limitation. Appl Environ Microbiol 68:1665–1673

Suzuki K, Liu H, Saino T, Obata H, Takano M, Okamura K, Sohrin Y, Fujishima Y (2002) East-west gradients in the photosynthetic potential of phytoplankton and iron concentration in the subarctic Pacific Ocean during early summer. Limnol Oceanogr 47:1581–1594

Takaichi S, Shimada K, Ishidsu J-I (1988) Monocyclic cross-conjugated carotenal from an aerobic photosynthetic bacterium *Eryhtrobacter longus*. Photochemistry 27:3605–3609

Takaichi S, Shimada K, Ishidsu J-I (1990) Carotenoid from the aerobic photosynthetic bacterium *Erythrobacter longus*: β-caroteme and its hydroxyl derivates. Arch Microbiol 153:118–122

Takaichi S, Furuhata K, Ishidsu J-I, Shimada K (1991) Carotenoid sulphates from the aerobic photosynthetic bacterium *Erythrobacter longus*. Photochemistry 30:3411–3415

Tamura K, Dudley J, Nei M, Kumar S (2007) MEGA4: Molecular Evolutionary Genetics Analysis (MEGA) Software Version 4.0. Mol Biol Evol 24:1596–1599

Tang K, Zong R, Zhang F, Xiao N, Jiao N (2010) Characterization of the photosynthetic apparatus and proteome of *Roseobacter denitrificans*. Curr Microbiol 60:124–133

Van Heukelem L, Thomas CS (2001) Computer-assisted high performance liquid chromatography method development with applications to the isolation and analysis of phytoplankton pigments. J Chromatogr A 910:31–49

Wagner-Dobler I, Biebl H (2006) Environmental biology of the marine *Roseobacter* lineage. Ann Rev Microbiol 60:255–280

Wyman M (1992) An in vivo method for the estimation of phycoerythrin concentrations in marine cyanobacteria (*Synechococcus* spp.). Limnol Oceanogr 37:1300–1306

Yurkov VV, Beatty JT (1998) Aerobic anoxygenic phototrophic bacteria. Microbiol Mol Biol Rev 62:695–724

Yurkov V, Csotonyi JT (2009) New light on aerobic anoxygenic phototrophs. In: Hunter N, Daldul F, Thurnaner MC, Beatty JT (eds) The purple phototrophic bacteria. Springer Science + Business Medio B. V, Berlin, pp 31–55